https://ntrs.nasa.gov/search.jsp?R=19850026410 2020-03-20T16:53:28+00:00Z

General Disclaimer

One or more of the Following Statements may affect this Document

- This document has been reproduced from the best copy furnished by the organizational source. It is being released in the interest of making available as much information as possible.

- This document may contain data, which exceeds the sheet parameters. It was furnished in this condition by the organizational source and is the best copy available.

- This document may contain tone-on-tone or color graphs, charts and/or pictures, which have been reproduced in black and white.

- This document is paginated as submitted by the original source.

- Portions of this document are not fully legible due to the historical nature of some of the material. However, it is the best reproduction available from the original submission.

Produced by the NASA Center for Aerospace Information (CASI)

NSG-7653

QUASIPERIODIC OSCILLATIONS IN BRIGHT GALACTIC-BULGE X-RAY SOURCES

BY

F. K. LAMB, N. SHIBAZAKI, M. A. ALPAR, AND J. SHAHAM

(NASA-CR-176138) QUASIPERIODIC OSCILLATIONS IN BRIGHT GALACTIC-BULGE X-RAY SOURCES (Illinois Univ., Urbana-Champaign.) 32 p HC A03/MF A01 CSCL 03A

N85-34723

Unclas
G3/89 22150

RECEIVED
NASA STI FACILITY
ACCESS DEPT.

UNIVERSITY OF ILLINOIS AT URBANA-CHAMPAIGN

DEPARTMENT OF PHYSICS

LOOMIS LABORATORY OF PHYSICS

1110 W. GREEN STREET

URBANA, ILLINOIS 61801

P/85/8/132

Submitted to Nature, May 7, 1985; accepted August 13, 1985.

QUASIPERIODIC OSCILLATIONS IN BRIGHT GALACTIC-BULGE X-RAY SOURCES

F. K. Lamb[*+], N. Shibazaki[*], M. A. Alpar[*‡], and J. Shaham[||]

Departments of [*] Physics and [+] Astronomy, University of Illinois at Urbana-Champaign, 1110 W. Green Street, Urbana, Illinois 61801, USA

[||]Department of Physics and Columbia Astrophysics Laboratory Columbia University, 538 W. 120th Street, New York, New York 10027, USA

Quasiperiodic oscillations with frequencies in the range 5-50 Hz have recently been discovered in X-rays from two bright galactic-bulge sources and Sco X-1. We propose that these sources are weakly magnetic neutron stars accreting from disks in which the plasma is clumped. The interaction of the magnetosphere with clumps in the inner disk causes oscillations in the X-ray flux with many of the properties observed.

Quasiperiodic oscillations have recently been discovered in X-rays from the bright galactic sources GX 5-1,[1,2] Cyg X-2,[3,4] and Sco X-1.[5,6] The frequency f_p of the oscillations varies from 20 to 36 Hz in GX 5-1, 28 to 43 Hz in Cyg X-2, and from 6-17 Hz in Sco X-1. In all the available data on GX 5-1 and Cyg X-2, f_p shows a strong positive correlation with the 1-10 keV count rate. The FWHM Δf_p of the peak in averaged power spectra varies from 4

---

‡ Present address: Research Institute for Basic Sciences, P.O. Box 74, Gebze, Kocaeli, Turkey.

PACS #'s: 97.10.Ha, 97.60.Gb, 97.60.Jd, 97 80.Gm, 97.80.Jp

to 13 Hz in GX 5-1 and from 12 to 20 Hz in Cyg X-2, depending on the count rate, with relative widths $\Delta f_p/f_p$ in the range 0.21-0.60. For Sco X-1, only the 5-15 keV count rate is available; f_p is strongly positively correlated with this count rate during 10-20 minute quiescent intervals between flaring episodes but appears to vary erratically during transitions to extended low states. The FWHM of the peak in the Sco X-1 power spectrum varies from 1 to 10 Hz. All three sources show substantial red noise. In GX 5-1 the rms fractional intensity variation caused by the quasiperiodic oscillations and that caused by the red noise both remain approximately constant as the source intensity increases, except perhaps at the highest intensities observed where the variation may be less. In Cyg X-2, on the other hand, the fractional variation caused by the oscillations remains approximately constant but that caused by the red noise increases as the intensity increases. Finally, in Sco X-1 the red noise down to the lowest frequencies so far explored is relatively weak when the oscillations are clearly present but becomes stronger when the source is most intense.

Here we suggest that these sources are weakly magnetic neutron stars accreting from Keplerian disks in which the plasma is clumped. Interaction of the magnetosphere with clumps in the inner disk causes the mass accretion rate and hence the X-ray intensity to vary at a harmonic of the beat frequency given by the difference between the rotation frequency of the star and the rotation frequency of the inner disk. [This idea has been suggested previously as a possible explanation for some of the quasiperiodic oscillations observed in cataclysmic variables (ref. 7; D. Lamb and Warner, private communication)]. The low harmonics of this beat frequency are comparable to the oscillation frequencies observed in GX 5-1,[8,9] Cyg X-2, and Sco X-1 for neutron star spin rates ~ 100 Hz, dipole magnetic fields ~ 10^9 G, and accretion rates ~ 10^{18} g s^{-1}. Such spin rates and dipole magnetic field

strengths are consistent with the hypothesis that systems like these are progenitors of the millisecond rotation-powered pulsars.[8] In addition, for neutron stars rotating near their equilibrium spin rates the low harmonics of this beat frequency vary with accretion rate in a manner similar to the observed variations of the oscillation frequency with X-ray intensity.[9]

We show that the power spectra given by a simple version of this model are very similar to the spectra reported in GX 5-1 and Cyg X-2. In particular, red noise at frequencies below that of the quasiperiodic oscillations is a logical consequence of the model. If all clumps in the inner disk contribute to the oscillations and if the properties of the clumps and the nature of their interaction with the magnetosphere remain unchanged, the strength of the red noise is proportional to that of the quasiperiodic oscillations, as observed in GX 5-1. If not, the strength of the red noise may increase even as the strength of the oscillations decreases, as observed in Cyg X-2 and Sco X-1. We present calculations which show that X-ray pulsations caused by beaming and rotation of the neutron star are strongly suppressed relative to quasiperiodic oscillations produced according to the present model, under the conditions thought to exist in bright galactic bulge sources. Several observational tests of the model are described.

Physical Model

The plasma flow pattern around a weakly magnetic neutron star accreting from a Keplerian disk at near the Eddington critical rate is expected to be similar to that around supermassive black holes in galactic nuclei accreting at near-critical rates.[10-12] The inner disk is radiation-pressure-dominated, unlike the inner disks surrounding canonical accretion-powered pulsars with dipole magnetic fields $\sim 10^{12}$ G. The luminosity of the inner disk is supplied in part by release of gravitational binding energy as the disk plasma spirals

in, and in part by radiation from the neutron star. The pressure of the radiation leaving the inner disk alone implies a disk height $h > 1.5(\dot{M}/\dot{M}_E)R$, where $\dot{M}_E$ is the mass flux corresponding to the critical accretion luminosity from the central star and R is the radius of the star. As a result, the magnetosphere is surrounded by a thick ($h \sim r$) plasma torus containing cooler, denser plasma with a scale height $h_c << h$ (see Fig. 1). A central corona and mass loss via a wind are expected due to heating of the surface of the disk by acoustic flux, magnetic flaring, and radiation from the neutron star.[13,14] In Sco X-1, the existence of radio lobes[15] is direct evidence for mass ejection from the system.

The plasma in the inner disk is expected to be spatially inhomogeneous as a result of three mechanisms that can cause clumping. First, vertical eruption of magnetic flux carried inward and amplified by the accretion flow creates strong spatial inhomogeneities in the density and magnetic field strength.[14,16] Second, for near-critical accretion rates, the disk-magnetosphere boundary lies only a few stellar radii from the surface of the neutron star; under these conditions, the inner disk is expected to be thermally unstable to the formation of clumps.[17-20] Third, the relative motion of magnetospheric and disk plasma drives the Kelvin-Helmholtz instability to large amplitudes near the inner edge of the disk, where the disk plasma is partially confined by the pressure of the magnetospheric field (ref. 21; Aly, Ghosh, & Lamb, reported in ref. 22).

Assuming that the cooler, denser plasma dominates the mass flux onto the neutron star, the disk ends where $B_p B_\phi \delta \approx \rho_c v_r r \Omega_B h_c$.[23] Here B_p and B_ϕ are the poloidal and toroidal components of the magnetospheric field, δ is the width of the boundary layer, ρ_c and v_r are the density and radial velocity of the plasma in the boundary layer, and the beat frequency $\Omega_B = \Omega_c - \Omega_s$ is the

difference between the angular velocity Ω_c of the plasma clumps and the rotation frequency Ω_s of the star (see Fig. 2). We expect $\Omega_c \approx \Omega_{KO}$, the Keplerian angular velocity at the radius[23] $r_0 = 0.52\mu^{4/7}(2GM)^{-1/7}\dot{M}^{-2/7}$ of the boundary layer. Here μ and M are the magnetic moment and mass of the star and $\dot{M}$ is the mass flux through the boundary layer. The spread in beat frequencies within the boundary layer is then $\Delta\Omega_B \approx |\partial\Omega_K/\partial r|_0\delta = 1.5(\delta/r_0)\Omega_{KO}$.

In the boundary layer, plasma clumps drift radially inward as they lose angular momentum by interaction with each other, with the surrounding gas, and with the stellar magnetic field. Plasma is stripped from the clumps by interaction with the magnetospheric field and plasma. Important mechanisms are likely to include stripping by surface stresses resulting from the Kelvin-Helmholtz instability[25] or by reconnection of magnetic flux in the clump with the stellar flux,[9] perhaps in a manner analagous to the reported[26] stripping of plasma from comets as they move through regions of alternating field direction in the solar wind. Once stripped, plasma is quickly brought into corotation with the neutron star and accretes to the stellar surface, producing X-rays there.

Unless the stellar field is axisymmetric, aligned with the rotation axes of disk and star, and centered in the star, the interaction of a given clump with the magnetosphere is greater at some stellar azimuths than at others. As a result, the rate at which plasma is stripped from the clump is greater at some azimuths than others (see Fig. 3). We refer to the stellar azimuth(s) at which the stripping rate is greater for a given clump as the special direction(s) for that clump. The pattern of the special directions and the steepness of the variation of the stripping rate with azimuth affect the harmonic content of the X-ray intensity waveform produced by the clump. For a pattern of special directions with k-fold symmetry, the pattern of mass flux to the stellar surface and hence the X-ray waveform repeats with frequency Ω_R

= $k\Omega_B$ ($k = 1, 2, 3, \ldots$). Suppose, for example, that the rotation axis of the star is aligned with that of the disk but its magnetic axis is tilted with respect to its rotation axis For a boundary layer magnetic field that is perfectly dipolar, the magnetic pressure on a clump is $\propto 1+3\cos^2(\Omega_B t+\phi)$, where ϕ is the phase of the clump. Thus, if the rate at which plasma is stripped from clumps is determined entirely by the magnetic stress acting on the clumps, $k = 2$. For the same geometry, reconnection of the magnetospheric field previously entrained by the clumps with the local magnetospheric field varies with frequency $2\Omega_B$, also giving $k = 2$. However, if there is the slightest asymmetry between the two magnetic poles, $k = 1$, even though most of the power in the clump waveform may be at $2\Omega_B$. Reconnection to the local magnetospheric field of a component of the magnetic field of a clump that remains fixed in the corotating frame (due, for example, to the magnetospheric interaction with the clump) varies with frequency Ω_B, giving $k = 1$. As long as the field in the boundary layer is nearly dipolar, the power in the principal peak of the power spectrum typically dominates that at the first overtone, due to the smoothness of the dipole field pattern. Even if the stripping rate varies as steeply as $\cos^6[(\Omega_B t+\phi)/2]$, the power in the first overtone is only 16% of that in the fundamental.

If the pattern of radiation from the neutron star is not axisymmetric in the disk plane at the inner disk, scattering of radiation into the line of sight by clumps in the inner disk will create a periodic anisotropy in the radiation from the system, causing some modulation of the X-ray intensity seen by a distant observer. However, we expect this effect to be much less important than modulation of the mass flux to the stellar surface for several reasons, including the small solid angle subtended by the clumps at the neutron star, the very weak beaming expected from these neutron stars, and the

suppression of modulation due to anisotropic radiation by the plasma surrounding the neutron star. The latter two effects are discussed in more detail below.

Power Spectrum

The theory of random processes (see, for example, Rice[27]) can be used to calculate the power density spectrum of the X-ray intensity time series I(t) produced by the collection of clumps orbiting within the boundary layer. The X-ray intensity waveform produced by exactly N clumps may be written

$$I_N(t) = I_0 + \sum_{i=1}^{N} F(t-t_i;\phi_i) , \qquad (1)$$

where I_0 is a possible constant intensity, $F(t;\phi)$ is the waveform contributed by a single clump, and ϕ_i is the azimuthal phase of the ith clump at the time it enters the boundary layer. Quite generally, an arbitrary clump waveform may be expanded in harmonics of the beat frequency:

$$F(t;\phi) = [A + \sum_{n=1}^{\infty} B_n \cos\{n(2\pi f_B t + \phi) - \alpha_n\}] G(t), \qquad (2)$$

where $f_B = \Omega_B/2\pi$, α_n is the phase of the nth harmonic in the clump waveform, and G(t) is an envelope function that describes the overall shape of the waveform. A, B_n, α_n, and ϕ may be treated as random variables. Equation (2) holds even if the special directions are different for each clump, as long as they have the same symmetry and remain fixed in the frame of the star.

The power spectrum produced by the clumps depends on whether they enter the boundary layer at random times, whether their positions are correlated, and whether stripping of a clump occurs independently of the presence of other clumps nearby. For simplicity, we assume initially that correlations are absent; later we indicate the effects that such correlations would have.

Assuming that the number of clumps entering the boundary layer in the

observing interval is Poisson distributed, that ϕ_i is uniformly distributed, and that t_i and ϕ_i are uncorrelated, the expected power density spectrum of the time series (1) is

$$\langle P(f)\rangle = 2\langle I\rangle^2\delta(f) + 2\langle I\rangle + 2\langle I\rangle^2\,\gamma_{RN}^2 g(f) + \langle I\rangle^2 \sum_{n=1}^{m} \gamma_n^2 [g(f-nf_B) + g(f+nf_B)] \tag{3}$$

where $\langle I\rangle = I_0 + \langle N\rangle\langle A\rangle$ is the mean intensity, $\gamma_{RN}^2 = \langle N\rangle\langle A^2\rangle/2\langle I\rangle^2$, and $\gamma_n^2 = \langle N\rangle\langle B_n^2\rangle/4\langle I\rangle^2$. The structure function $g(f)$ is proportional to $|s(f)|^2$, where $s(f)$ is the Fourier transform of $G(t)$, but is normalized to unit area. It includes the 'lifetime' broadening (FWHM $\Delta f_L = 1/\pi\tau$) produced by the finite duration τ of the waveform contributed by a single clump.

The first term in equation (3) is the power at zero frequency due to the mean intensity while the second is the power density in the Poisson noise produced by photon statistics. The term proportional to $g(f)$ describes the red noise caused by time variations in the photon arrival rate. The presence of this additional noise follows immediately from the fact that the mean X-ray intensity contributed by each clump is positive and persists only for a finite time. All clumps that contribute to the oscillations necessarily contribute to the red noise. (The converse need not be true.) The terms proportional to $g(f-nf_B)$ describe the power density near nf_B produced by the oscillating X-ray intensity. For most waveforms, the terms proportional to $g(f+nf_B)$ may be neglected.

The repetition frequency of the oscillations in the X-ray wave train contributed by a single clump varies in time as the clump drifts inward across the boundary layer since its angular velocity varies with radius. This variation may be described by introducing a distribution of clump angular velocities. In addition, one expects a distribution of clump lifetimes rather than a single lifetime. These effects may be included by averaging equation

(3) over the expected distribution $\rho(f_B,\tau)$, which yields equation (3) with g everywhere replaced by $\bar{g} = \langle \rho g \rangle$. In the case of the oscillation terms, $\bar{g}$ equals $\tilde{g}_n$, the convolution of g with $\rho(f_B/n;\tau)/n$. Thus, if g and ρ may both be approximated by a Lorentzian (or Gaussian) profile, $\tilde{g}$ is a Lorentzian (or Gaussian). After this averaging, $\langle P(f) \rangle$ has peaks at $f_n = n\bar{f}_B$, where $\bar{f}_B$ is the frequency $\langle \rho f_B \rangle$, with FWHMs that are, loosely speaking, the sum of Δf_L and the width $n\Delta f_S \approx n\Delta\Omega_B/2\pi$ caused by velocity shear in the boundary layer. The power in the zero-frequency, red noise, and oscillating components is

$$P_0 = \int_0^{0+\varepsilon} \langle P(f) \rangle df = \langle I \rangle^2, \tag{4}$$

$$P_{RN} = 2\langle I \rangle^2 \gamma_{RN}^2 \int_0^\infty \bar{g}(f)\, df = \langle I \rangle^2 \gamma_{RN}^2 \tag{5}$$

and

$$P_n = \langle I \rangle^2 \gamma_n^2 \int_0^\infty \tilde{g}_n(f) df \approx \langle I \rangle^2 \gamma_n^2 \int_{-\infty}^\infty \tilde{g}_n(f) df = \langle I \rangle^2 \gamma_n^2 . \tag{6}$$

Thus, the rms fractional intensity variation caused by the red noise is $\gamma_{RN} = (P_{RN}/P_0)^{1/2}$ while that due to the oscillation at f_n is $\gamma_n = (P_n/P_0)^{1/2}$. For comparison, the fractional modulation in the oscillation at f_n (defined as half the peak-to-peak intensity variation of a sinusoid of equivalent power, divided by $\langle I \rangle$) is $m_n = \sqrt{2}\gamma_n$.

If $F(t;\phi)$ is a pure sinusoid ($B_n \neq 0$ for only one value of n, say m) and if the stripping of each clump occurs independently, $A > B_m$ for each clump, since then the X-ray intensity contributed by each clump must be positive at all times. This implies $\gamma_{RN} > \gamma_m$. If the assumptions concerning t_i and ϕ_i made in deriving equation (3) are also satisfied, equations (5) and (6) show that P_m is at most $0.5P_{RN}$. If $F(t;\phi)$ is a pure sinusoid but ϕ_i is not uniformly distributed, the oscillation and red noise Fourier amplitudes interfere, introducing an additional phase-dependent term $\propto \mathrm{Re}\, g^*(f)g(f-mf_B)$ in equation

(3) that changes the shape of the spectrum near $mf_B/2$ but alters P_m/P_{RN} by only a small amount. Such interference usually also occurs if ϕ_i is correlated with t_i. However, for some correlations between ϕ_i and t_i this interference is absent if t_i is uniformly distributed, but the oscillation Fourier amplitudes contributed by different clumps interfere constructively unlike the red noise amplitudes, causing P_m to exceed P_{RN} by a large factor. Alternatively, if $F(t;\phi)$ is a pure sinusoid but is scaled by certain functions $H(\phi)$, such as $\cos^{2q}(\phi)$ for $q>>1$, P_m can approach P_{RN}. Finally, if $F(t;\phi) \propto \cos^{2q}[(2\pi mf_B t-\phi)/2]$, with $q>3$, P_m exceeds P_{RN}. The power density $\langle P(f)\rangle$ used here is related to the power density P_j defined in ref. 28 by the expression $P_j = \langle P(f)\rangle/\langle I\rangle$. (Note that although the second of eqs. (1) of ref. 28 displays the angular frequency ω, P_j in this equation is normalized to power per circular frequency interval.)

Suppose the principal peak in the power spectrum is at the frequency $f_p = n\bar{f}_B$. According to the physical model described above, as the mass flux $\dot{M}$ through the boundary layer changes, the radius r_0 of the layer changes also, causing a change in Ω_{K0}. Since f_s may be treated as constant for times much shorter than the timescale for changes in the spin rate of the neutron star, here $\sim 10^5$ years, the change in Ω_{K0} results in a change in f_p. Consider now the relation between f_p and the X-ray intensity I observed at earth in a given energy band. If no mass was lost from the system after passing through the boundary layer, if all observed X-rays came from the surface of the neutron star, and if there were no changes in the geometry of the emission region or the X-ray spectrum, I would be proportional to $\dot{M}$. However, in the bright galactic-bulge sources there are strong indications[29-32] that these conditions are not satisfied. We therefore consider the more general relation $I = I_E(\dot{M}/\dot{M}_E)^\beta$, where $I_E = \eta L_E$ in terms of the Eddington luminosity $L_E = 1.257 \times 10^{38}(M/M_\odot)$ ergs s^{-1} for hydrogen plasma. Here η is a conversion factor that

takes into account the distance, as well as geometric and bolometric corrections. (If I is the EXOSAT 1-10 keV count-rate, D_8 is the distance in units of 8 kpc, and if the source emits isotropically with a spectrum like GX 5-1, $\eta \approx 1.42\times10^{-35}D_8^{-2}$ ct erg^{-1}; cf. ref. 2) Then (cf. ref. 9)

$$f_p = n[a(I/I_E)^{3/7\beta} - f_s], \tag{7}$$

where $a = 1.57\times10^3(B_d/10^9G)^{-6/7}(R/10^6cm)^{-15/7}(M/M_\odot)^{5/7}$. Here B_d is the dipole component of the stellar magnetic field. A frequently reported quantity[2,4] is the logarithmic derivative of f_p with respect to the X-ray count-rate which, in this model, is given by (cf. ref. 9)

$$\alpha = \frac{d\ell n\ f_p}{d\ell n\ I} \approx \frac{3}{7\beta}\ \frac{1}{(1 - \omega_s)}, \tag{8}$$

where $\omega_s = \Omega_s/\Omega_{KO}$ is the fastness parameter.[21]

X-Ray Pulsations

X-ray pulsations produced by rotation of the neutron stars in the bright galactic-bulge X-ray sources have not yet been detected. The canonical view is that the magnetic fields of these neutron stars are so weak ($B_d < 10^6$ G) that they do not channel the accretion flow (see, e.g., ref. 33). In contrast, the model of quasiperiodic oscillations developed here requires neutron star magnetic fields $\sim10^9$ G in the bright bulge sources exhibiting such oscillations. Such fields could channel the accretion flow to some extent[34] and hence could produce some X-ray beaming. However, in the context of the present model there are three distinct physical effects that, for distant observers, suppress pulsations at the rotation frequency of the neutron star.

First, X-ray beaming from the neutron star surface is much less in the present model than in canonical accretion-powered pulsars. The relatively

weak magnetic field of the neutron star is less effective in channeling the accretion flow.[34] Radiation pressure forces within the magnetosphere produced by the high luminosity of the star support the accreting plasma,[35] causing it to settle over a large fraction of the star's surface. Evidence that accreting plasma falls over a substantial fraction of the surface comes from analyses of the hard component in the spectrum, which yield emitting areas comparable to the surface area of a neutron star.[4,31,32,36] Such a broad distribution of accreting plasma and the resulting broad X-ray beam produces modulation that is weak and is at relatively high harmonics of the rotation frequency of the neutron star. The modulation may be further weakened by gravitational bending of the X-ray photon ray paths in the strong gravitational field of the neutron star (K. Wood, private communication; see also ref. 37).

Second, the torus and corona around the neutron star (see Fig. 1) tend to destroy X-ray pulsations caused by beaming while leaving unaffected the quasiperiodic oscillations caused by modulation of the accretion rate. The existence of central coronae with dimensions $\sim 10^7$ cm and optical depths ~4-12 is strongly indicated by analyses of the X-ray spectra of the bright galactic-bulge sources.[4,32,38] After passing through a corona of electron scattering optical depth $\tau_{es} > 4$, the observed fractional modulation due to beaming, m_{obs}, is much less than m_{star}, where m_{star} is the fractional modulation that would be observed in the absence of the corona (for calculations that illustrate this behavior in a different context, see Figs. 3 and 5 of ref. 39). In the present model, the quasiperiodic oscillations are due to variations in the mass flux onto the neutron star. Thus, even if the emission from the neutron star were perfectly isotropic, these oscillations would still be observable. The fractional modulation produced by variation of the mass flux is unaffected if the mean time for photons to propagate through the corona is less than the

oscillation period, i.e., if $r_{cor}\tau_{es}/c < 1/\nu_p$ (see Fig. 4). Taking $r_{cor} = 10^7$ cm, $\tau_{es} = 10$, and $m_{star} = 0.1$ as an example, the fractional modulation at the rotation frequency would be <<1 whereas the fractional modulation in 30 Hz quasiperiodic oscillations would be unaffected, i.e., equal to the fractional modulation in the accretion rate.

Third, the thick torus and disk corona surrounding the neutron star prevent us from seeing X-rays coming directly from the neutron star except when our line-of-sight is close to the star's rotation axis, in which case modulation due to beaming is further weakened. The inner disk is expected to be both geometrically thick and optically thick to electron scattering (see discussion of Fig. 1). There is strong evidence that in bright galactic-bulge sources the outer disk is also both geometrically and optically thick.[41-43] As a result, we do not see X-rays coming directly from the neutron star except in systems with small inclinations.[33] Assuming that the rotation axis of the neutron star is perpendicular to the plane of the disk, such systems are viewed from near the rotation axis, a direction in which modulation due to beaming is absent.

If our analysis of the weakness of X-ray pulsations at the rotation frequency of the neutron star is correct, such pulsations should be most apparent in sources with relatively low intrinsic luminosities and optically thin coronae.

Discussion

The variation of oscillation frequency with X-ray intensity depends on the properties of the neutron star and the gross properties of the accretion flow, whereas the shape of the power density spectrum is determined by the physics of the boundary layer. Consider first the change in oscillation frequency.

Equation (7) fits the variation in f_p with I observed[2] in GX 5-1 for a substantial range of neutron star magnetic fields and stellar spin rates, as illustrated by Table 1 (see also[2,9]). Models 1-3 assume that f_p is the fundamental beat frequency; Models 4-6, that f_p is the first overtone. All assume that the photons in the so-called 'soft' component of the spectrum come from the inner disk (see Fig. 1) whereas the photons in the 'hard' component come initially from near the surface of the neutron star[12,31,32,36] (but see[4]). In Models 1 and 4 the 40% observed change in 1-10 keV X-ray intensity is assumed to be due mostly to a change in the fraction of the radiation from the neutron star that is scattered into our line of sight, with the change in the mass flux through the boundary layer (and hence the accretion luminosity) only 10%. In Models 2 and 5 the change in intensity is assumed to be due mostly to variation of the mass flux, which changes by 40%, whereas in Models 3 and 6 the change in the mass flux (80%) is much larger than the change in the X-ray intensity, as could be the case if most of the photons from the neutron star do not reach us. For each value of β, $\dot{M}_1$ was fixed by assuming that a 1-18keV EXOSAT count rate of 4850 ct s^{-1} corresponds to the critical luminosity and noting that the count rate I_1 corresponding to $\dot{M}_1$ is 2427 ct s^{-1} (we note, however, that the value of η quoted above yields a luminosity at 4850 ct s^{-1} of $1.9L_E$ for D = 8 kpc and $M = 1.4M_\odot$). $\dot{M}_2$ is then determined by I_2, which is 3401 ct s^{-1}. Given the range in mass accretion rate, the dipole component of the neutron star magnetic field B_d ($=2\mu/R^3$) is determined entirely by the variation Δ_p of f_p from I_1 to I_2. Once B_d is fixed, the stellar rotation frequency f_s is determined by f_p. Both B_d and f_s are quite sensitive to the assumed variation in $\dot{M}$. The fastness parameter ω_s, which is independent of n, ranges from 0.95 for Models 1 and 4 to 0.51 for Models 3 and 6.

Equation (7) can also be fit to the f_p-I correlation observed in Cyg X-2

as well as that observed in Sco X-1 during local minima of the flaring state, for similar neutron star magnetic fields and spin rates (see also[4,6]). The currently allowed variation in the parameters among different models of the same source is greater than the variation from source to source, for these three systems.

Indirect support for the beat-frequency model is provided by the fact that the neutron star rotation rates and magnetic field strengths inferred from it are consistent with the idea[44-46] that systems like GX 5-1 and Cyg X-2 are progenitors of the millisecond rotation-powered pulsars.[2,8,9] Obviously, detection of weak pulsations at the predicted neutron star spin rate would provide the most direct evidence in favor of this model. As Table 1 shows, measurement of f_s would determine the harmonic number n and tightly constrain the change in mass flux through the boundary layer. However, it may be possible to constrain the beat-frequency model even without direct knowledge of f_s by extending the f_p-I relation to higher intensity and increasing the precision of the measurements, since the shape of the theoretical f_p-I curve is different for different values of the parameters.

Consider now the evidence provided by the shape of the power spectrum. In the following discussion we assume that the average power spectra reported for GX 5-1 and Cyg X-2 accurately reflect the shapes of the individual spectra that have been averaged. If this is not the case, the model parameters appropriate to these sources will of course be different from those inferred here.

The width of the peak due to quasiperiodic oscillations depends on Δf_L and $n\Delta f_s$ whereas the shape of the red noise depends only on Δf_L. Thus, fits of model spectra to observed spectra provide estimates of both quantities. Figure 5 compares one spectrum observed in GX 5-1 with two model spectra. In GX 5-1, the power in the oscillations is comparable to the power in the red

noise down to the lowest frequencies so far explored, when the oscillations are most prominent. Recall that if the X-ray intensity waveform produced by each clump is sinusoidal and the assumptions leading to equation (3) are satisfied, P_m can be at most $0.5P_{RN}$. In the sinusoidal model P_1 does indeed equal $0.5P_{RN}$, but half the noise power is at frequencies below the lowest frequency so far explored, due to the distribution of clump lifetimes. In the other model, the waveform is not a pure sinusoid, with the result that P_1 is $1.1P_{RN}$. As Figure 5 illustrates, these two models can be adjusted to fit the GX 5-1 observations over the frequency range so far studied. For the non-sinusoidal model, an acceptable fit is not possible for $\Delta f_S > 0.5$ Hz. The fact that the lifetime broadening inferred from the red noise spectrum accounts for a substantial fraction of the width of the peak at f_p in the averaged power spectra suggests that the widths of the peaks in the individual spectra are not very different.

Note that if the clumps are the dominant source of accreting plasma ($I_0 << \langle N\rangle\langle A\rangle$) and $\langle A^2\rangle \sim \langle A\rangle^2$, one can estimate the number of clumps in the boundary layer, since then $\langle N\rangle \sim 1/2\gamma_{RN}^2$. The result is $\langle N_a\rangle = \langle N_b\rangle \sim 30$ for the sinusoidal model and $\langle N\rangle \sim 120$ for the other. Both models can also be adjusted to give good agreement with the spectra reported[4] in Cyg X-2. Because the spectra they predict have different low-frequency behavior and different harmonic content, future observations can distinguish between them.

Analysis of the harmonic content of the oscillations can help to determine whether the observed peak is the fundamental beat frequency or an overtone. If f_p represents the fundamental (n=1), power may be expected at integer multiples of f_p but not at $f_p/2$. If instead f_p is the first overtone (n=2), some power may be expected at the fundamental beat frequency $f_p/2$. The distribution of power among the harmonics of f_p also constrains the physics of

the process by which plasma is stripped from the clumps: the weaker the overtones, the more linear the process. The absence of a prominent feature at $2f_p$ indicates that the variation in stripping rate cannot be as steep as $\cos^{2q}[(2\pi f_B t+\phi)/2]$ with $q>4$.

The ratio of the power P_p at the principal oscillation frequency to the power P_{RN} in the red noise depends on the harmonic content and fractional modulation of the X-ray waveform produced by a single clump. The relatively large apparent value of this ratio (~1) in GX 5-1 and Cyg X-2 suggests a large fractional modulation. If such a large value is confirmed when the spectrum is extended to lower frequencies, it would indicate substantial azimuthal variation of the conditions in the boundary layer, favoring magnetospheric geometries in which the axis of the stellar field is tilted by a substantial angle or is offset from the center of the star by a substantial distance. In both sources P_p is observed to vary. If the clump waveform remains unchanged as P_p varies, P_{RN} is proportional to P_p, as observed in GX 5-1.[2] More generally, P_{RN} need not be proportional to P_p and may even increase as P_p decreases, as has been reported in Sco X-1[3] and Cyg X-2.[6] If the changes in P_p/P_{RN} are due to variations in the shape of the clump waveform, the relative strengths of the harmonics of f_p must also change, whereas if they are due entirely to changes in the fractional modulation of the waveform, the relative strengths must remain unchanged. Thus, precise measurements of the power spectrum can show which effect is more important.

The ratios P_p/P_0 and P_{RN}/P_0 are related to the rms fractional modulation of the waveform produced by all the clumps involved. The substantial (~6-10%) fractional modulations observed[2,4,6] favor models like the present one in which the modulated X-rays come from the neutron star, since that is where the bulk of the gravitational energy becomes available.[12] If most of the photons from the star reach us without gaining or losing appreciable energy, the

oscillations and red noise should be most prominent in the spectral component that comes from the neutron star. However, photons from the star will suffer an energy shift $\Delta E \approx E$ after only $(m_e c^2/k_B T_r)$ scatterings, if $T_r > T_e$, or $(m_e c^2/k_B T_e)$ scatterings, if $T_r < T_e$.[47] Thus, those photons from the star that reach us only after scattering through a plasma of optical depth $\tau \sim 10$ (for $T_r \approx 2$ keV and $T_e \sim$ 1-7 keV[4,32,38]), will have energies characteristic of the temperature of the plasma rather than that of the surface of the star. As shown above, the fractional modulation of the oscillations in the flux of these photons is unaffected for a plasma of this optical depth if its dimension is $< 10^7$ cm. In any case, the X-ray spectral dependence of the variation in intensity due to the red noise at frequencies not too far below f_p should be similar to that of the variation due to the quasiperiodic oscillations.

From the narrowness of the observed peak at f_p one can show as follows that the lifetime τ of a clump is long compared to the time for it to fall freely across the boundary layer, and hence that its angular velocity Ω_c must be Keplerian. The time required for a clump to cross the boundary layer in free-fall is[21] $\Delta t_{ff} \sim (1/\Omega_{K0})\cdot(\delta/r_0)^{1/2}$, where Ω_{K0} is the Keplerian angular velocity at r_0. Now $\Delta f_p > \Delta f_L = 1/\pi\tau$. Further, $f_p \sim (n\Omega_{K0}/2\pi)\cdot(1-\omega_s)$. Thus,

$$\frac{\tau}{\Delta t_{ff}} \sim \Omega_{K0}\tau\left(\frac{r_0}{\delta}\right)^{1/2} >> \Omega_{K0}\tau \sim \frac{2/n}{1-\omega_s}\,\frac{f_p}{\Delta f_p} \sim 10\text{-}200 \ . \qquad (9)$$

Given that Ω_c is closely Keplerian in the boundary layer, $\Delta f_p > n\Delta f_S = (n/2\pi)\cdot|\partial\Omega_c/\partial r|_0\delta = (3n/4\pi)\Omega_{K0}(\delta/r_0)$. Using this relation, one can show

$$\delta/r_0 < (2/3)(1-\omega_s)(\Delta f_p/f_p) \sim 10^{-1}\text{-}10^{-2} \ . \qquad (10)$$

Noting that $v_r \sim \delta/\tau$, one can also show

$$v_r/v_\phi < (n/3)(1-\omega_s)^2(\Delta f_p/f_p)^2 \sim 10^{-2}\text{-}10^{-4} \quad . \tag{11}$$

An independent estimate of τ is provided by the noise component of the spectrum, which must flatten below the critical frequency $f_c \approx 1/2\pi\tau$.

The quasiperiodic oscillations seen in Sco X-1 are observed to disappear altogether at times.[5,6] If they are correctly interpreted in terms of the present model, the fact that Δf_p has been observed to increase substantially during a transition from flaring to quiescence (Priedhorsky, private communication) suggests that conditions within the boundary layer are variable. The broadening could be due to increased shear or a shorter mean clump lifetime. Fits of equation (3) to the red noise and the oscillation peak can indicate which is more important. If conditions in the inner disk change sufficiently, the formation of clumps could be inhibited. We note also that if the density and radius of the corona above the inner disk increase to the point that $r_{cor}\tau_{es}/c >> 1/f_p$, the oscillations will be destroyed by electron scattering in the corona. In this case, changes in the X-ray spectrum characteristic of the development of a denser and more extensive corona should be observable. Thus, simultaneous measurements of the X-ray spectrum and power spectrum can help to determine the relative importance of these processes.

The present model suggests a natural explanation for the 'dips' occasionally seen in GX 5-1 when the X-ray intensity is near its minimum value.[31] In our model the radius r_0 of the inner edge of the disk is quite close to the centrifugal radius r_c. Thus, when the mass accretion rate is near its minimum value, r_0 may briefly equal or exceed r_c. When this happens, the mass flux from the inner edge of the disk to the neutron star temporarily ceases[21,34] and one observes only the 'soft' component from the disk.[31]

In closing, we emphasize that the model described here may be relevant to other galactic-bulge X-ray sources. For example, the 2 Hz oscillations seen[48] in long flat-top bursts from the Rapid Burster may be a beat frequency phenomenon. If so, our model implies that the Rapid Burster has a surface magnetic field ~ 10^{11} gauss, assuming f_s ~ 20 Hz. The absence of a so-called 'soft' component in the X-ray spectrum of the Rapid Burster (Y. Tanaka, private communication) may also indicate that this source has a significant magnetosphere. If the 10^{-3} Hz oscillations reported[49] in the 8 sec accretion-powered pulsar 4U1626-67 also prove to be an example of this phenomenon,[9] it would demonstrate that the thermally unstable region of the inner disk is not essential to the development of clumping, since such a region is absent in this source. Our model then gives an estimate of the surface magnetic field of ~ 10^{13} gauss. This estimate is independent of the similar estimate derived from the observed spin-up rate,[50] but consistent with it. Finally, we note that the present work, when scaled appropriately, may be relevant to some of the quasiperiodic oscillations observed in some cataclysmic variables.[7,51,52]

We thank G. Hasinger, M. van der Klis, W.H G. Lewin, and W. Priedhorsky for discussing their observations in advance of publication; F. Cordova, S. Hayakawa, E.P.J. van den Heuvel, D. Lamb, J. van Paradijs, J. Swank, N. White, and G. Zylstra for helpful discussions; and B. Fortner for help in producing the figures. This research was supported in part by NSF under grant PHY 80-25605 at Illinois and by NASA under grant NSG 7653 at Illinois and grants NAGW-567 and NAG 8-497 at Columbia.

REFERENCES

1. van der Klis, M., Jansen, F., van Paradijs, J., Lewin, W.H.G., Trümper, J. & Sztajno, M. IAU Circular No. 4043 (1985).
2. van der Klis, M., Jansen, F., van Paradijs, J., Lewin, W.H.G., van den Heuvel, E.P.G., Trümper, J. E. & Sztajno, M. Nature, in press.
3. Hasinger, G., Langmeier, A., Sztajno, M. & White, N. E. IAU Circular No. 4070 (1985).
4. Hasinger, G., Langmeier, A., Sztajno, M., Trümper, J., Lewin, W.H.G. & White, N. E. Nature, submitted (1985).
5. Middleditch, J. & Priedhorsky, W. IAU Circular No. 4060 (1985).
6. van der Klis, M., Jansen, F., White, N., Stella, L. & Peacock, A. IAU Circular No. 4068 (1985).
7. Warner, B. in Cataclysmic Variables and Related Objects (ed. Livio, M. & Shaviv, G.) 155-172 (Reidel, 1983).
8. Alpar, M. A. & Shaham, J. IAU Circular No. 4046 (1985).
9. Alpar, M. A. & Shaham, J. Nature, in press.
10. Eardley, D. M., Lightman, A. P., Payne, D. G. & Shapiro, S. L. Astrophys. J. 224, 53 (1978).
11. Rees, M. J. in Extragalactic Radio Sources, Proc. IAU Symposium No. 97 (ed. Heeschen, D. S. & Wade, C. M.) 211 (Reidel, 1982).
12. Lamb, F.K. in Evolution of Galactic X-Ray Binaries (ed. Brinkmann, W., Lewin, W.H.G., & Trümper, J.), in press.
13. Begelman, M. C., McKee, C. F. & Shields, G. A. Astrophys. J. 271, 70 (1983).
14. Stella, L. & Rosner, R. Astrophys. J. 277, 312 (1984).
15. Geldzahler, B. J., Fomalont, E. B., Hilldrup, K. & Corey, B. E. Astr. J. 86, 1036 (1981).
16. Pustilnik, L. A. & Shvartsman, V. F. in Gravitational Radiation and Gravitational Collapse (ed. C. DeWitt-Morette) 213 (Reidel, 1974).

17. Pringle, J. E., Rees, M. J. & Pacholczyk, A. G. Astr. Astrophys. 29, 179 (1973).

18. Lightman, A. P. & Eardley, D. M. Astrophys. J. (Letters) 187, L1 (1974).

19. Hoshi, R. Publ. Astron. Soc. Japan 36, 785 (1984).

20. Taam, R. E. & Lin, D.N.C. Astrophys. J. 287, 761 (1984).

21. Ghosh, P. & Lamb, F. K. Astrophys. J. 232, 259 (1979).

22. Aly, J.-J. In Magnetospheric Phenomena in Astrophysics, Proceedings of the Conference in Taos, New Mexico, August 1984, in press.

23. Ghosh, P. & Lamb, F. K. Astrophys. J. 234, 296 (1979).

24. Ghosh, P., Lamb, F. K. & Pethick, C. J. Astrophys. J. 217, 578 (1977).

25. Arons, J. & Lea, S. Astrophys. J. 235, 1016 (1980).

26. Brandt, J. C. & Niedner Astrophys. J. 223, 655 (1978).

27. Rice, S. O. Bell System Technical Journal 23 & 24 [reprinted in Selected Papers on Stochastic Processes (ed. Wax, N.) 133 (Dover, 1954)].

28. Leahy, D. A., Darbro, W., Elsner, R. F., Weisskopf, M. C., Sutherland, P. G.,Kahn, S., & Grindlay, J. Astrophys. J. 266, 160 (1983).

29. Shibazaki, N. & Mitsuda, K. In High Energy Transients in Astrophysics, AIP Conference Proceedings No. 115 (ed. Woosley, S. E.) 63 (New York, American Institute of Physics, 1984).

30. Mitsuda, K. Ph.D. Thesis, University of Tokyo (1984).

31. Mitsuda, K., et al. Publ. Astron. Soc. Japan 36, 741 (1984).

32. White, N. E., Peacock, A. & Taylor, B. G. Astrophys. J., in press (1985).

33. Milgrom, M. Astr. Astrophys. 67, L25 (1978).

34. Lamb, F. K., Pethick, C. J. & Pines, P. 1973, Astrophys. J. 184, 271 (1973).

35. Davidson, K. Nature Phys. Sci. 246, 1 (1973)

36. Kendziorra, E., Collmar, W., Brunner, H. Staubert, R., & Pietsch, W. In Proceedings of the 18th ESLAB Symposium on X-Ray Astronomy, Scheveningen, The Netherlands, November 5-9, 1984, in press.

37. Pechenick, K. R., Ftaclas, C. & Cohen, J.M. Astrophys. J. 274, 846 (1983).

38. Hirano, T., Hayakawa, S., Kunieda, H., Makino, F., Masai, K., Nagase, F. & Yamashita, K. Publ. Astron. Soc. Japan 36, 769 (1984).

39. Hertz, P., Joss, P. C. & Rappaport, S. Astrophys. J. 224, 614 (1978).

40. Chang, K. M. & Kylafis, N. D. Astrophys. J. 265, 1005 (1983).

41. White, N. E. & Holt, S. S. Astrophys. J. 257, 318 (1982).

42. McClintock, J. E., London, R., Bond, H. & Grauer, A. Astrophys. J. 258, 245 (1982).

43. Fabian, A. C., Guilbert, P. W., and Ross, R. R. Mon. Not. R. astr. Soc. 199, 1045 (1982).

44. Alpar, M. A., Cheng, A. F., Ruderman, M. A. & Shaham, J. Nature 300, 728 (1982).

45. Radhakrishnan, V. & Srinivasan, G. Curr. Sci. 51, 1096 (1982).

46. Fabian, A. C., Pringle, J. E., Verbunt, F. & Wade, K. A. Nature 301, 222 (1983).

47. Sunyaev, R. A. & Titarchuk, L. G. Astr. Astrophys. 86, 121 (1980).

48. Y. Tawara, S. Hayakawa, S., Kunieda, H., Makino, F. and Nagase, F. Nature 299, 38 (1982).

49. Li, F., Joss, P.C., McClintock, J.., Rappaport, S. & Wright, E.L. Astrophys. J. 628 (1980).

50. Henrichs, H. In Accretion-Driven Stellar X-Ray Sources (ed. W.H.G. Lewin & E.P.J. van den Heuvel) 393 (Cambridge Univ. Press, 1983).

51. Patterson, J. Astrophys. J. 234, 978 (1979).

52. Cordova, F. A. & Mason, K. O. In Accretion-Driven Stellar X-Ray Sources (ed. W.H.G. Lewin & E.P.J. van den Heuvel) 147 (Cambridge Univ. Press, 1983).

TABLE 1

REPRESENTATIVE MODELS OF GX 5-1*

MODEL	n	B_d	f_s	P_s	β	$\dot{M}_1$	$\dot{M}_2$	r_{01}	r_{02}
1	1	5.5	384	2.6	3.6	0.82	0.91	3.1	3.0
2	1	19.9	88	11.4	1.0	0.50	0.70	7.4	6.7
3	1	31.6	39	26.0	0.58	0.30	0.55	11.1	9.4
4	2	12.3	191	5.2	3.6	0.82	0.91	4.9	4.7
5	2	44.6	44	22.7	1.0	0.50	0.70	11.7	10.6
6	2	70.8	19	51.8	0.58	0 30	0.55	17.6	14.9

*All models assume a 1.4 $M_\odot$ neutron star of radius 10^6 cm and are fit to f_p = 20.07 Hz and Δ_p = 16.8 Hz. The symbols and their units are: harmonic number n, dipole component of the stellar magnetic field B_d (10^9 G), stellar spin frequency f_s (Hz), rotation period P_s (ms), mass flux at 2427 ct s^{-1} $\dot{M}_1$ ($\dot{M}_E$), mass flux at 3403 ct s^{-1} $\dot{M}_2$ ($\dot{M}_E$), boundary layer radius r_{01} (10^6 cm) at $\dot{M}_1$ and r_{02} (10^6cm) at $\dot{M}_2$. $\dot{M}_E$ is the Eddington luminosity of the neutron star.

FIGURE CAPTIONS

Fig. 1 Side view of the plasma flow pattern expected around a weakly magnetic neutron star accreting from a disk at near the critical rate.[12] Shown are the neutron star (black circle), magnetosphere (dark shaded circle), dense clumped plasma (dark shading), torus (moderate shading), and central corona (light shading); θ is the opening angle of the throat of the torus. Photons (long arrows) enter the torus both from the clumped plasma and from the neutron star; photons from the neutron star emerging along the axis of the torus are scattered by the throat walls and plasma in the throat and corona. Mass is lost from the disk and torus via a wind (short arrows).

Fig. 2 Magnetospheric (Ω_s) and clump (Ω_c) angular velocities in the inner disk and boundary layer, showing the meaning of the quantities Ω_B, $\Delta\Omega_B$, r_0, and δ. Inside r_{co}, plasma is in generalized corotation[24] with the star; also indicated is the centrifugal radius r_c at which plasma in the disk corotates with the star. The width of the boundary layer has been greatly exaggerated for clarity.

Fig. 3 Schematic drawing of the narrow boundary layer at the inner edge of the disk, from which plasma accretes onto the surface of the neutron star. The spiral depicts the trajectory of a given clump, as seen in a frame corotating with the star. In this frame, the clump moves with azimuthal velocity $r(\Omega_c(r)-\Omega_s)$ and radial velocity v_r. Plasma is stripped from the clump continuously, but the rate of stripping depends on the azimuthal position of the clump. The sections of the trajectory where the stripping rate is high for this particular clump (the 'special directions' referred to in the text) are depicted with heavy lines whereas those where it is low are depicted with light lines. In this example, the frequency of the observed oscillations is equal to the fundamental beat frequency $\Omega_B = \Omega_c(r)-\Omega_s$. If

instead the pattern of special directions has two-fold symmetry, the transfer rate is also high along those sections of the trajectory indicated with heavy dashed lines and the frequency of the observed oscillations is the first overtone of the fundamental beat frequency.

Fig. 4 Fractional modulation in quasiperiodic oscillations seen by a distant observer as a function of coronal radius r_{cor} and oscillation frequency f_p, for $\tau_{es} = 10$. Heavy curve: uniform sphere; light curve: thin shell. For the example given in the text, $\log(r_{cor} f_p/c) = -2$. (Adapted from ref. 40.)

Fig. 5 Top: Power spectrum observed in GX 5-1 at 2277-2486 counts s^{-1}, when $f_p = 20.07$ Hz and $\Delta f_p = 4.2$ Hz.[2] The spectrum to the right of the peak has been smoothed. A visual estimate of the 1σ error at $2f_p$ is shown. Bottom: Power spectrum calculated for a model with $F \propto \cos^6[(2\pi f_B t+\phi)/2]$ and a single clump lifetime (solid curve: $\gamma_1 = 2.5\gamma_2 = 15\gamma_3 = 1.1\ \gamma_{RN} = 6.7\times10^{-2}$, $f_1 = 20.07$ Hz, $\tau = 0.085$s, $\Delta f_{S1} = 0.47$ Hz; the relative widths $\Delta\ln(f)$ of the peaks at f_1, $2f_1$, and $3f_1$ are 0.21, 0.12, and 0.085, respectively) and a model with $F \propto 1+\cos(2\pi f_B t+\phi)$ and two clump lifetimes (dashed curve: $\gamma_{RNa} = \gamma_{RNb} = \sqrt{2}\gamma_{1a} = \sqrt{2}\gamma_{2b} = 6.3\times10^{-2}$, $f_1 = 20.07$ Hz, $\tau_a = 50$ s, $\tau_b = 0.085$s, $\Delta f_{Sa} = \Delta f_{Sb} = 2.6$ Hz). Both models assume the assumptions leading to equation (3) are satisfied, a clump waveform $G(t) = \Theta(t)\exp(-t/\tau)$, and a Lorentzian angular velocity distribution, which gives $g_i(f) = 2\tau_i[1+(2\pi f\tau_i)^2]^{-1}$ and $\tilde{g}_{ni}(f-f_n) = 2\tau_i(1+\pi n\Delta f_S\tau_i)\cdot([2\pi(f-f_n)\tau_i)]^2+[1+\pi n\Delta f_S\tau_i]^2)^{-1}$. Note the marked difference in the low-frequency behavior of the two calculated spectra and the much smaller difference in harmonic content.

ORIGINAL PAGE IS
OF POOR QUALITY

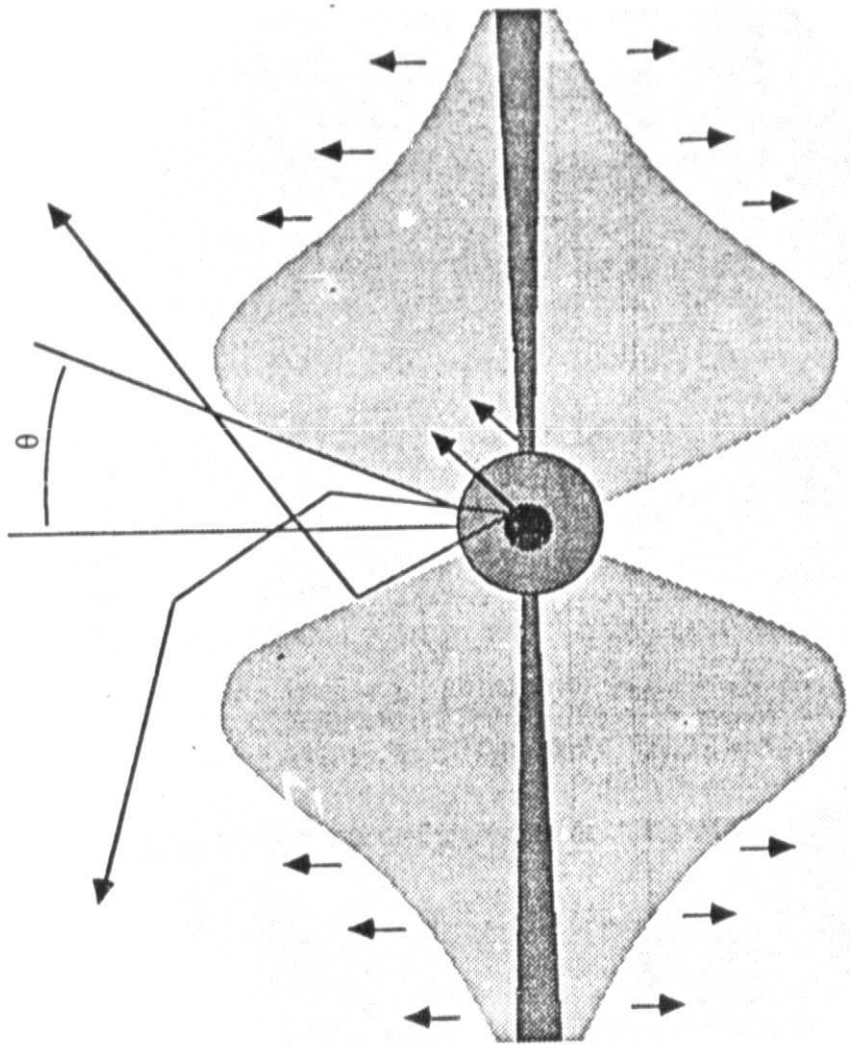

Figure 1

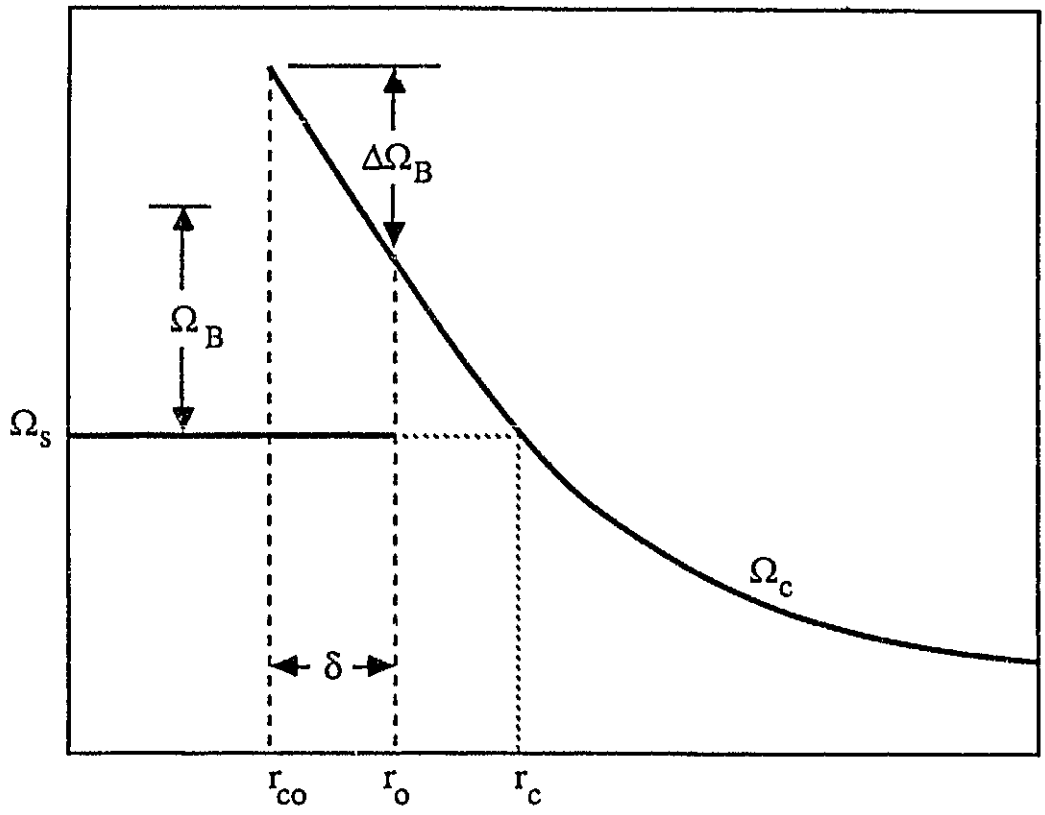

Figure 2

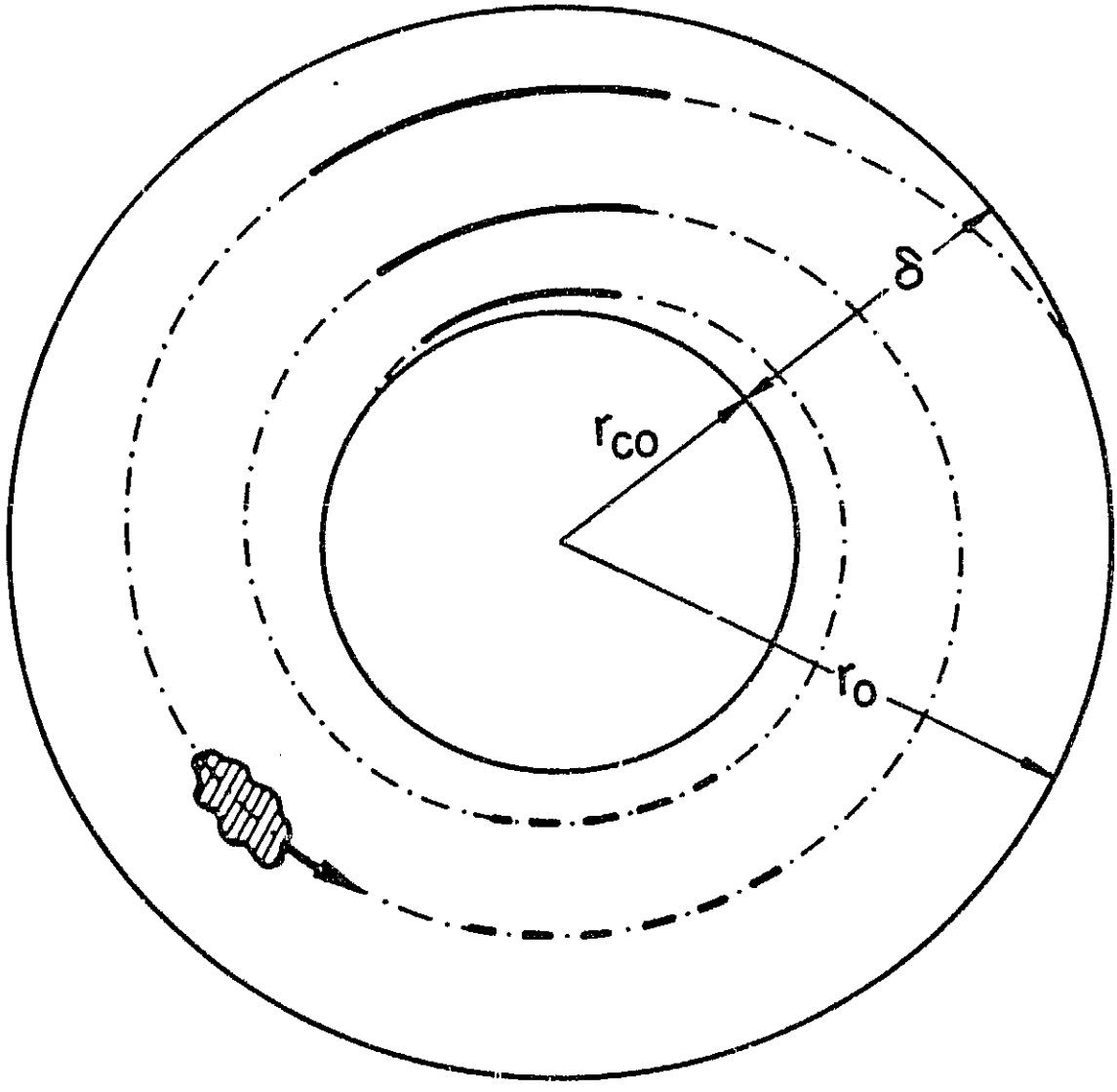

Figure 3

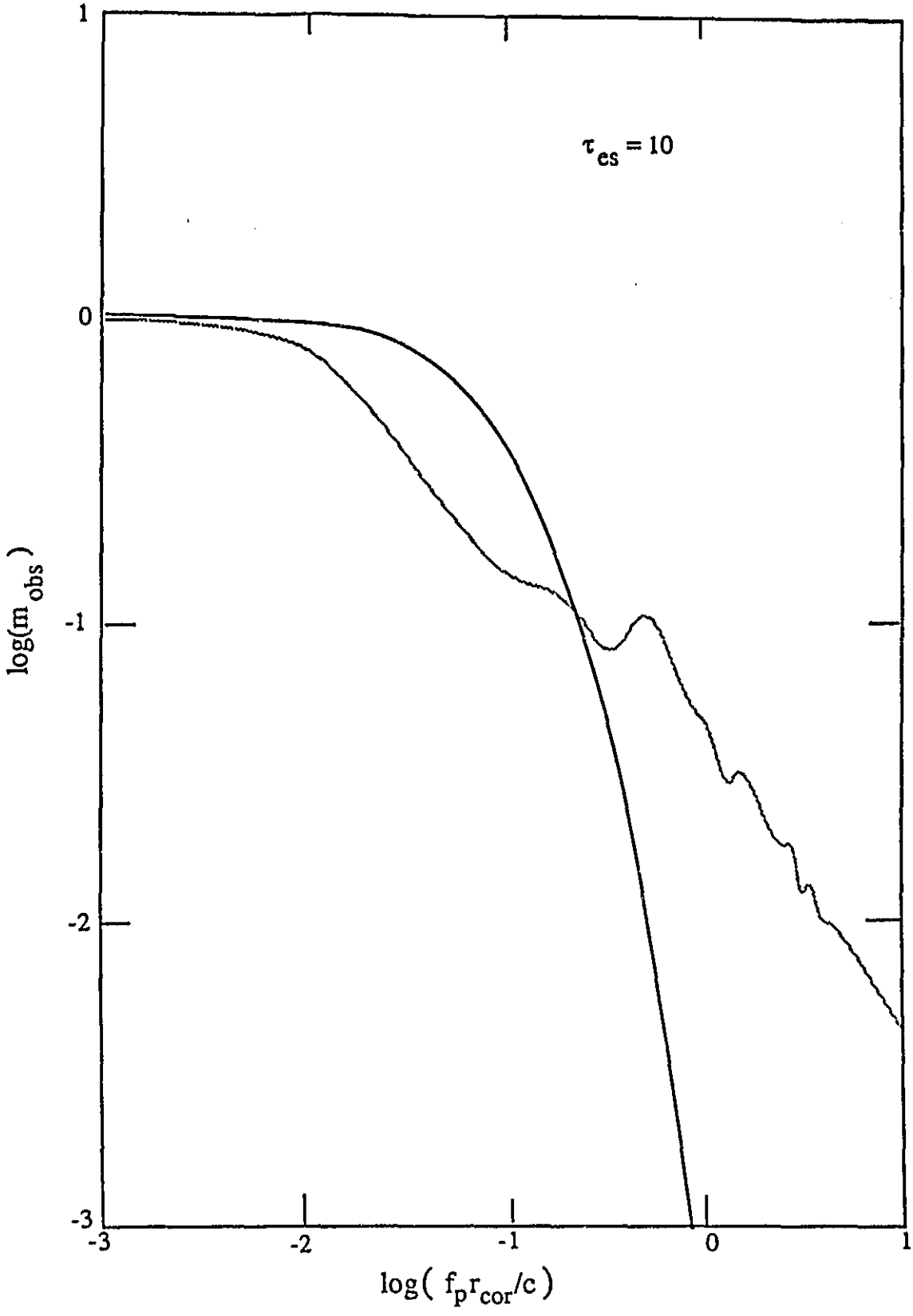

Figure 4

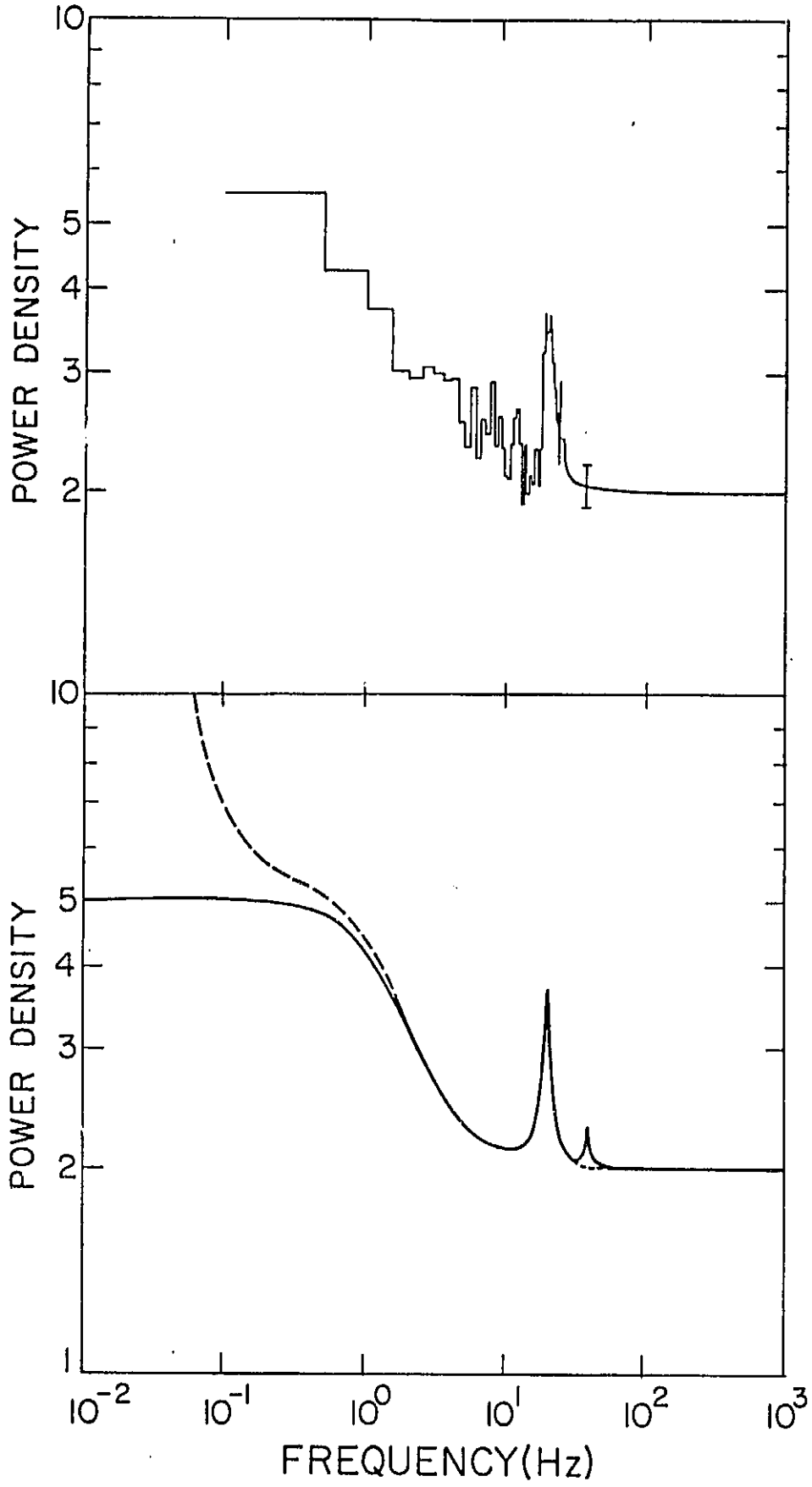
10
5
4
3
2
POWER DENSITY
10
5
4
3
2
1
POWER DENSITY
10^{-2}
10^{-1}
10^{0}
10^{1}
10^{2}
10^{3}
FREQUENCY(Hz)

Figure 5